

Modeling Structural Abnormalities in Equivalent Dipole Layer Based ECG Simulations

Manon Kloosterman¹, Machteld J Boonstra¹, Folkert W Asselbergs¹, Peter Loh¹, Thom F Oostendorp², Peter M van Dam¹

¹University Medical Centre Utrecht, Department of Cardiology, Utrecht, The Netherlands

²Donders institute for Brain, Cognition and Behaviour, Radboud University Medical Centre, Nijmegen, The Netherlands

Abstract

The relation between abnormal ventricular activation and corresponding ECGs still requires additional understanding. The presence of disease breaks the equivalence in equivalent dipole layer-based ECG simulations. In this study, endocardial and epicardial patches were introduced to simulate abnormal wave propagation in different types of substrates. The effect of these different types of substrates on the QRS complex was assessed using a boundary element method forward heart/torso and a 64-lead body surface potential map (BSPM). Activation was simulated using the fastest route algorithm with six endocardial foci and QRS complexes corresponding to abnormal patch activation were compared to the QRS complexes of normal ventricular activation using correlation coefficient (CC). Abnormal patch activation affected both QRS morphology and duration. These QRS changes were observed in different leads, depending on substrate location. With insights obtained in such simulations, risk-stratification and understanding of disease progression may be further enhanced.

1. Introduction

The electrocardiogram (ECG) is widely used as a diagnostic tool to provide insight in the electrical activity of the heart. In progressive cardiomyopathy, the shape and magnitude of the measured body surface potentials (BSP) change over time.[1] The relation between abnormal ventricular activity on corresponding ECG abnormalities still requires additional understanding which can be obtained through invasive electroanatomic mapping and ECG simulation studies. Using the latter, slight changes in underlying ventricular activation can be simulated, achieving more detailed insight and understanding of electrical substrates. The *ECGsim* program is such a well-known interactive ECG simulation program.

Two types of models are required to simulate the ECG; a cardiac source model, representing electrical currents generated by ventricular cells, and a volume conductor model representing the effect of these generated currents on the ECG.[2] The equivalent dipole layer (EDL) is such a cardiac source model. The EDL is positioned at the endocardial and epicardial surface bounding the myocardium. The local source strength at each element of this surface model is defined by the local transmembrane potential. Changing local depolarization and repolarization times result in changes in the simulated ECG.[3]

The EDL model assumes that the myocardial tissue beneath the bounding surface is homogeneous and thus, the presence of locally diseased myocardium breaks the equivalence of the dipole layer. To restore the equivalence, in order to adequately simulate abnormal substrate activation, an additional boundary between healthy and diseased myocardium was incorporated, referred to as patches. In this simulation study, we explore the use of such patches representing different types of substrates to simulate abnormal wave propagation and to study their effect on the ECG.

2. Methods

2.1. Simulation of normal activation

We used a CT-based anatomical model (57y male) with a 64-lead ECG set-up. The anatomical model contained the triangulated surface meshes of the ventricular myocardium, blood pools, thorax and lungs with the following assigned conductivities: 0.2 S/m, 0.6 S/m, 0.4 S/m and 0.2 S/m respectively. The discrete transfer matrix was computed using the boundary element method from each triangle of the discretized ventricular surface towards each observation point at or within the torso.[4]

The EDL was used as a cardiac source model.[3] First, the described patient specific (57y male) anatomical model

was used to simulate BSP corresponding to approximated normal activation by using six foci in combination with the fastest route algorithm.[5] The source strength at each node is proportional to the local transmembrane potential with its shape defined by δ and ρ , the local depolarization and repolarization time respectively (Figure 1A).[3]

2.2. Simulation of diseased myocardium

To simulate abnormal substrate activation, boundaries were incorporated between healthy and diseased myocardium, thus the healthy myocardium was separated from diseased by embedding patches within the ventricular model. At three different locations, endocardial and epicardial patches were embedded within the ventricular model and in the right ventricular outflow tract (RVOT) only an epicardial patch was embedded (Figure 1B).

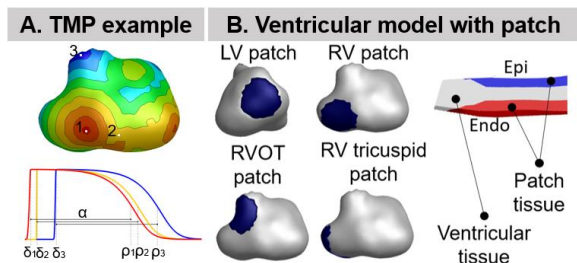


Figure 1. A. Simulated activation sequences from red (early) to blue (late) with corresponding local transmembrane potentials. With α indicating transmembrane potential duration, δ activation timing and ρ repolarization timing. B. CT-based ventricular model with patches (bleu region). Patches were embedded within the ventricular model (red endocardial, blue epicardial).

Patch activation sequences were computed using the fastest route algorithm together with a set propagation velocity. Different types of patch activation were simulated (e.g. delay and dyssynchronous) to assess the effect on simulated BSP. Delayed patch activation was simulated by reducing patch propagation velocity from 0.85 m/s (normal) to 0.25 m/s (severe delay). Dyssynchronous patch activation was simulated adding Gaussian noise (0-90 ms). Depending on the electrical connection (continuous or discontinuous) between ventricular and patch tissue (Figure 2), nodes electrically in contact with the ventricular model were assigned the same activation timing as the ventricular nodes. Three types of connections were simulated; patch nodes directly opposing ventricular nodes were either (1) fully electrically connected with the ventricular model (continuous), (2) the outer ring of the patch was connected to the ventricular model (discontinuous type 1), or (3) the latest 25% of the outer ring was connected to the ventricular model (discontinuous type 2). Specifically, for each model with both an endocardial and epicardial patch, 45 simulations were performed and for the model with only

an epicardial patch 18. Different combinations of patch activation and connection types (Figure 2) were assigned to patches separately and together.

We compared BSP of all abnormal cases to the simulated BSP corresponding to normal ventricular activation by comparing QRS duration and morphology. Most affected leads were identified as the lead with the lowest Pearson's correlation coefficient (CC). Data was assessed for normality and normally distributed variables were reported as mean \pm standard deviation and non-normally distributed data as median [interquartile range]. Differences between groups was assessed using student's-t-test for normally distributed data and Mann-Whitney-U test for non-normally distributed data and significance was assumed when p-value was below 0.01.

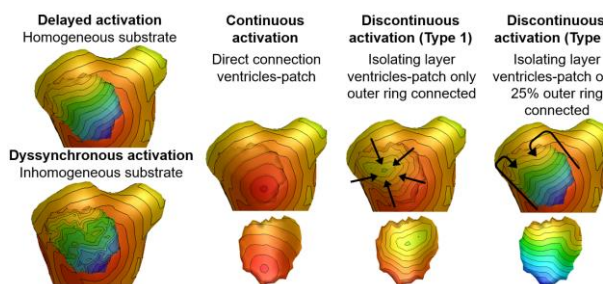


Figure 2. Different types of patch simulations (delayed, dyssynchronous, continuous and discontinuous). Activation sequences are displayed as local activation timing maps from red (early) to blue (late).

2.3. Clinical case

Brugada Syndrome is characterized by the presence of fibrofatty tissue at the epicardial surface in the RVOT. In cases with Brugada syndrome, Ajmaline provocation results in increased activation wave disruption in the diseased area. To simulate Brugada, we created an epicardial patch in the RVOT wherein locally disrupted activation waves were simulated. Ajmaline provocation was simulated by further increasing local activation wave propagation in the patch and decreasing myocardial propagation velocity of both the healthy and diseased regions. Furthermore, current-to-load mismatch was simulated in the patch by locally decreasing transmembrane potential amplitudes. Specifically, epicardial transmembrane potentials were more decreased compared to the mid-myocardial ones.

3. Results

Distinct patch activation wave types affected both QRS morphology and duration (Figure 3). Dyssynchronous substrate resulted in significantly more evident changes in both QRS morphology and duration compared to a delayed substrate (Figure 3, Table 1). Discontinuous patch activation due to an 'isolating' layer between patch and

normal ventricular myocardium (**Figure 4**), resulted in a patch activation initiated at the edge of the patch. The direction of activation through the patch differed depending on the connection between the ventricular myocardium and the patch. For a delayed patch, a significant difference was observed between a continuously delayed patch versus both delayed type 1 and 2 activation, whereas for the dyssynchronous patch, a significant difference between all groups was observed (**Table 1**). The presence of an epicardial versus endocardial patch resulted in an opposing electrical vector observed in BSP. Depending on substrate location, the agreement between QRS complexes was different amongst leads (**Figure 5**).

Table 1: Median correlation coefficient (CC_{med}) and interquartile range in QRS-CC for all simulations.

Protocol	QRS- CC_{med}
Delay + continuous	1.00 [0.99;1.00] $\pm^{\$}$
Delay + discontinuous Type 1	1.00 [1.00;1.00] *
Delay + discontinuous Type 2	1.00 [1.00;1.00] *
Dyssynchronous + continuous	0.97 [0.92;0.99] $\pm^{\$}$
Dyssynchronous + discontinuous Type 1	0.98 [0.93;1.00] $\pm^{\$}$
Dyssynchronous + discontinuous Type 2	0.98 [0.95;1.00] $\pm^{\$}$

Significant difference compared to delayed + continuous activation is denoted with * . Differences in the three connection types is assessed for delayed and dyssynchronous separately. Significant differences with type 1 activation is denoted with \pm and type 2 is denoted with $^{\$}$.

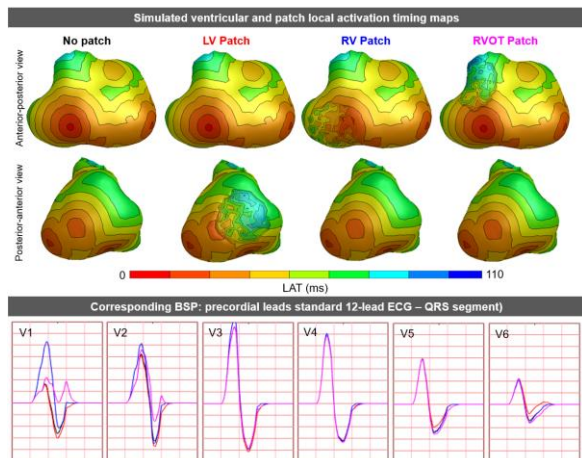


Figure 3. Abnormal patch activation and corresponding V1-V6. Myocardial conduction velocity was 0.85 m/s and of the patch 0.45 m/s. A dyssynchronous pattern was simulated by adding randomly to local activation times (0-30 ms).

The simulation of Ajmaline provocation in Brugada Syndrome (**Figure 6**) resulted in increased patch activation disruption. Consequently, increased R'-wave amplitude was observed. This, in combination with overall reduction in myocardial conduction velocity, resulted in increased QRS duration. By introducing a difference in epicardial and midmyocardial transmembrane amplitude, a potential difference over the patch was introduced, resulting in ST-

segment elevation (**Figure 6B**). Leads V1 and V2 of the standard 12-lead ECG were affected most and when assessing changes in the Brugada leads (**Figure 6C**), larger changes were observed.

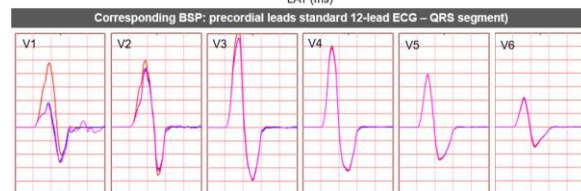
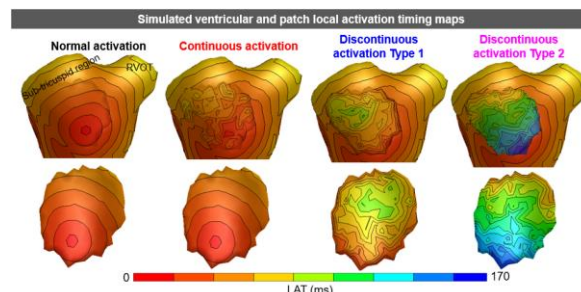


Figure 4. Abnormal patch activation and corresponding V1-V6. Myocardial conduction velocity was 0.85 m/s and of the patch 0.45 m/s. A dyssynchronous pattern was simulated by adding randomly to local activation times (0-30 ms) combined with different connection types.

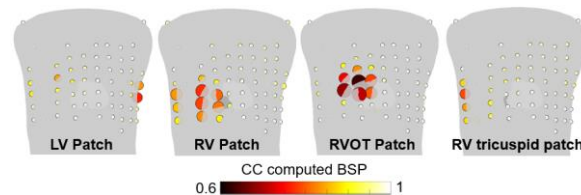


Figure 5: Effect of patch location on corresponding BSP. Mean \pm standard deviation of correlation coefficient (CC) per lead between normal and abnormal BSP is displayed. Each dot represents an electrode, the color representing average CC and the size magnitude in standard deviation.

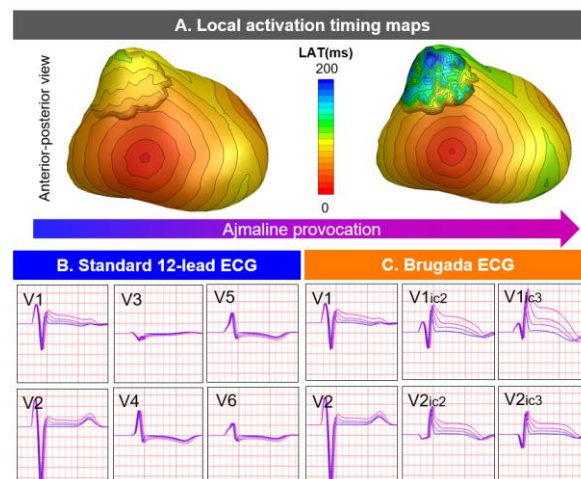


Figure 6 Ajmaline provocation in Brugada Syndrome. Progressively increasing QRS duration, changing QRS morphology and ST-segment elevation can be observed upon simulated ajmaline administration (blue to purple).

4. Discussion

In this study, we introduce a novel method to study the effect of different types of abnormal cardiac electrical activity on the ECG. We enable modeling of substrates consisting of both electrically active and inactive myocardium (*e.g.* healthy and fibrous myocardium) without breaking the equivalence of the dipole layer. We observed that a dyssynchronous substrate had a larger effect on QRS morphology compared to a delayed substrate, resulting in lower QRS-CC values. With the new simulation method, we obtained local activation timing map patterns similar to the described patterns of diseased areas assessed during invasive electro anatomic mapping studies.

In previous studies, transmural scar was modeled by creating a hole in the ventricular model to simulate regions without electrical activity. This however is not a correct representation of diseased regions, both for substrates as seen in old myocardial infarctions and inherited cardiomyopathies. Within diseased regions, both electrically active and inactive myocardium is present. With the introduced patches, a more representative model of such substrate and its effect on the ECG is provided.

With the method, insight in the effect of different substrate types on the ECG and most affected leads depending on substrate location is obtained. This information can in turn be used as prior knowledge for the detection of subtle disease progression in for example inherited cardiomyopathies like arrhythmogenic cardiomyopathy. The possible benefit of disease specific lead locations for the early identification of disease progression can be investigated which in turn may be used for improved risk-stratification.

Whereas this study mainly focused on the depolarization sequence and corresponding QRS complex, the method may also be used to study the effect of pathology on repolarization and corresponding ST-segment and T-wave, as showed with the Brugada case. Typical Brugada related clinical ECG changes in both the QRS complex and ST-segment were observed when simulating Ajmaline provocation. In future studies, we will focus on improving the model for repolarization, both in healthy and diseased myocardium.

The patches were modeled as separate source models which were electrically connected to the healthy ventricular tissue. It thus may also provide a way to investigate reentry circuits due to locally altered wave propagation properties due to local disease affecting ion channels. In the presented method, the effect of such circuits and the possibility of reentry should be explicitly simulated as the transmembrane potential is represented by the combination of three factors, one defining the slope of depolarization and two defining the leading and trailing slope of repolarization. Combining the EDL method with a cellular model to provide the ability to locally alter ion

currents which in turn affect the transmembrane potential, may provide a way to also study effects of regionally altered activation wave properties in subsequent beats.

Propagation velocity was modified to simulate different substrate types, but in the most severe cases of disease, it was set far below realistic physiological values (0.25 m/s). Furthermore, a linear relation between source strength of the patch and the percentage of electrically inactive cells in the diseased region was assumed, which should be further investigated. In our case of normal ventricular activation, a slurring S-wave in V6 was observed, which is normally not present in the healthy 12-lead ECG.

5. Conclusion

With the novel method, different types of myocardial disease with specific activation characteristics can be simulated. The method provides a new way to directly provide insight in the effect of different types of abnormal activation sequences on the ECG. The method may be used for teaching purposes to assess the relation of different types and locations of abnormal myocardial activation on ECG waveforms. In future studies, also the application of the method in the non-invasive estimation of activation in the presence of diseased myocardium will be researched.

Acknowledgements

This work was supported by the Dutch Heart Foundation (grant numbers CVON2015-12 eDETECT and QRS-Vision 2018B007)

References

- [1] Rautaharju PM, Park LP, Chaitman BR, Rautaharju F, Zhang Z-M. "The Novacode criteria for classification of ECG abnormalities and their clinically significant progression and regression" *J Electrocardiol.*, 31, 3, 157-87, 1998
- [2] van Dam PM, Oostendorp TF, van Oosterom A. "ECGSIM: Interactive Simulation of the ECG for Teaching and Research Purposes" *Computing in Cardiology* 37, 841-4, 2010
- [3] van Dam PM, Oostendorp TF, Linnenbank AC, van Oosterom A. "Non-invasive imaging of cardiac activation and recovery" *Annals of Biomed Eng.*, 37, 9, 1739-1756 2009
- [4] Oostendorp T, van Oosterom A. "The potential distribution generated by surface electrodes in inhomogeneous volume conductors of arbitrary shape" *IEEE Trans Biomed Eng.*, 38, 5, 409-17 1991
- [5] van Dam PM, Oostendorp TF, van Oosterom A. "Application of the fastest route algorithm in the interactive simulation of the effect of local ischemia on the ECG" *Med Biol Eng Comput.*, 47, 1, 11-20, 2009

Address for correspondence:

Manon Kloosterman

Heidelberglaan 100, 3584 CX Utrecht, The Netherlands

manon.kloosterman@live.com